2002

Visual and Lidar Observations of Noctilucent Clouds above Logan, Utah, at 41.7°N

Vincent B. Wickwar
Utah State University

M J. Taylor

J P. Herron

B A. Martineau

Recommended Citation
Wickwar, V. B., M. J. Taylor, J. P. Herron, and B. A. Martineau (2002), Visual and lidar observations of noctilucent clouds above Logan, Utah, at 41.7°N, J. Geophys. Res., 107(D7), 4054, doi:10.1029/2001JD001180.

JOURNAL OF GEOPHYSICAL RESEARCH, VOL. 107, NO. D7, 4054, 10.1029/2001JD001180, 2002

Visual and lidar observations of noctilucent clouds above Logan, Utah, at 41.7°N

Vincent B. Wickwar, Michael J. Taylor,[1] and Joshua P. Herron
Center for Atmospheric and Space Sciences, Utah State University, Logan, Utah, USA
Physics Department, Utah State University, Logan, Utah, USA

Bethany A. Martineau
Center for Atmospheric and Space Sciences, Utah State University, Logan, Utah, USA

Received 28 September 2000; revised 6 July 2001; accepted 13 July 2001; published 11 April 2002.

[1] Noctilucent clouds (NLCs) were observed from a midlatitude site (Logan, Utah) on the evenings of 22 and 23 June 1999 mountain daylight time. On both nights the clouds were seen for approximately an hour by experienced observers, and they were photographed. The NLC was also observed on the second evening for approximately an hour in the zenith with the Rayleigh-scatter lidar at the Atmospheric Lidar Observatory, which is operated by the Center for Atmospheric and Space Sciences on the campus of Utah State University. These observations enabled several of the properties of the cloud to be determined. They were within the range of those observed at higher latitudes, but notably the NLC was very weak and thin. These combined visual and lidar observations unequivocally support the identification of the cloud as a noctilucent cloud. The midlatitude location (41.74°N, 111.81°W) is ~10° equatorward of previous observations. This equatorward penetration is significant because of potential implications about global change or the global circulation. *INDEX TERMS:* 0305 Atmospheric Composition and Structure: Aerosols and particles; 0340 Atmospheric Composition and Structure: Middle atmosphere—composition and chemistry; 1640 Global Change: Remote sensing; *KEYWORDS:* climate change, noctilucent cloud, polar mesospheric cloud, Rayleigh-scatter lidar, mesosphere, Atmospheric Lidar Observatory

1. Introduction

[2] Past observations and reviews of noctilucent clouds [e.g., *Gadsden and Schroder*, 1989] and polar mesospheric clouds [*Thomas and Olivero*, 1989] indicate that they occur in summer at polar latitudes in the upper mesosphere between 80 and 86 km and are composed of ice crystals. (We assume that these represent the same phenomenon observed under different conditions.) Noctilucent clouds (NLCs) have usually been studied visually above the northern horizon during the long twilight periods near the end of summer from such locations as southern Alaska, Scotland, and Scandinavia. The equatorward extent of their penetration is considered to be ~50°N. (We have not found verifiable references in the published literature of previous observations equatorward of 50°N.) The equatorward extent for polar mesospheric clouds is similar or a little less. *Donahue et al.* [1972] show some detections from OGO 6 between 50° and 55° latitude, while *Thomas and Olivero* [1989] indicate that the equatorward detection threshold from the SME satellite was 55° latitude. For ice crystals to form at the low pressures of these altitudes, significant water vapor has to exist, and the temperature has to be extremely cold. Low temperatures in the polar summer mesosphere are understood in terms of the meridional component of the mesospheric circulation. It flows from summer to winter hemisphere at high altitude followed by subsidence heating in the winter hemisphere, and it flows from winter to summer hemisphere at lower altitudes followed by adiabatic cooling of the rising air in the summer mesosphere. The result of these dynamical effects is that the upper mesospheric temperature at polar latitudes is considerably colder in summer than in winter. The driving force for the mesospheric circulation is attributed to gravity waves generated in the troposphere, propagating upward, and depositing momentum in the mesosphere.

[3] Recently, NLCs have been detected in the zenith with lidars at several sites: Andenes, Norway, at 69.3°N [*Hansen et al.*, 1989] (also the location of the Andoya Rocket Range and, now, the Artic Lidar Observatory for Middle Atmosphere Research, ALOMAR); Sondrestrom, Greenland, at 67.0°N [*Thayer et al.*, 1995]; Juliusruh, Germany, at 54.6°N [*von Cossart et al.*, 1996]; Kühlungsborn, Germany, at 54°N [*Alpers et al.*, 2000]; and Aberystwyth, United Kingdom, at 52.4°N [*Thomas et al.*, 1994]. This technique has extended the ability to examine NLCs from near the horizon to overhead; to determine their altitude, altitude variations, and thickness; to characterize the particle "density" and size [*von Cossart et al.*, 1999]; and to observe them even in full sunlight [*von Zahn et al.*, 1998].

[4] In the past few years the impression has been that NLCs are being seen more frequently than in the past and at lower latitudes. This has led to the question, as discussed by *Thomas* [1996, and references therein], as to whether these sightings reflect a combination of an early indication of global warming from increased levels of CO_2 in the atmosphere (which produces cooling in the mesosphere) and of increased levels of mesospheric water vapor obtained from the oxidation of elevated levels of CH_4 in the atmosphere (which would increase the temperature at which NLCs form). In short, do these sightings provide an early warning of global climate change? Our unequivocal detection of a NLC from 41.7°N

[1]Formerly at Space Dynamics Laboratory, Utah State University, Logan, Utah, USA.

0148-0227/02/2001JD001180$09.00

Figure 1. Panoramic photograph of noctilucent clouds (NLCs) from Logan, Utah, at 10:30 P.M. MDT on 22 June 1999 (0430 UT on 23 June 1999). The photograph (taken by one of the authors, M. J. Taylor) was obtained using a Minolta SLR fitted with a 50 mm, $f/1.7$ lens, and Kodak 100 ASA color film exposed for ~10 s. See color version of this figure at back of this issue.

by a combination of visual sightings above the northern horizon and lidar detection in the zenith will certainly intensify this debate.

2. Observations

[5] The visual observations were carried out from the southeast side of Logan, looking north. This location is close to the Atmospheric Lidar Observatory (ALO) at 41.74°N and 111.81°W. On both 22 and 23 June 1999 MDT (23 and 24 June UT), NLCs were seen in evening twilight between ~9:45 and 10:45 P.M. MDT (0345 and 0445 UT), corresponding to local solar zenith angles (SZAs) of 97° and 105°, respectively. No NLCs were seen during the corresponding twilight period, between 4:10 and 5:12 A.M. MDT (1010 and 1112 UT) the following morning. On the second evening they were thinner than the night before but extended to higher elevation angles.

[6] The NLCs were photographed on both nights. On 23 June UT they were first photographed at 10:09 P.M. MDT, at which time they consisted of two distinct "patches" in the northwestern and northern sky containing fine wave-like structures at elevations up to ~5°. Figure 1 is a panoramic picture made from two successive images of the NLC at 10:30 P.M. MDT (0430 UT on 23 June 1999). It looks over the Utah State University (USU) campus when the Sun was at 103° SZA. The main NLC patch is to the right of image center and appears bright and silvery white with a blue hue. The second NLC patch is on the left side of the image and is less intense and smaller in area. A narrow bank of tropospheric clouds is present in the foreground with clear (blue) sky and patchy clouds at higher elevations. At far left is the green laser beam from the USU/Center for Atmospheric and Space Sciences (CASS) Atmospheric Lidar Observatory. (For reference, the top of the radio tower is at a 3.0° elevation angle.) These observations are discussed in more detail by *Taylor et al.* [2002].

[7] The lidar observations were carried out with a Rayleigh-scatter lidar with a power-aperture product of 2.77 W m^2 at 532 nm pointing in the zenith. It is a coaxial system composed of a Spectra Physics GCR-5 neodymium: yttrium/aluminum/garnet (Nd:YAG) laser operating at 30 Hz at 600 mJ per pulse at 532 nm and a 44-cm-diameter Newtonian telescope. The intense low-altitude returns are blocked by a rotating chopper and by an electronic gate for the cooled photomultiplier tube (Electron Tubes 9954B), which is gated on at 38 km, providing good data from below 45 km to above 90 km. This is essentially the system described by *Wickwar et al.* [1997, 2001]. The elemental sampling gate width is 250 ns or 37.5 m. However, the data reduction integrates over three gates, making the effective gate width 750 ns or 112.5 m. In the analysis a boxcar average can be performed over any multiple of 112.5 m, with the result returned every 112.5 m. With a laser beam divergence of <500 μrad, the horizontal spot size, or resolution, is <41 m at 82-km altitude. The elemental integration time is 2 min, and the data can be averaged over any multiple of 2 min.

[8] On the local evening for 23 June UT, although the laser beam is visible in Figure 1, no data were acquired because the laser beam and telescope were being aligned. By 0858 UT the lidar was obtaining good data and did so until 1108 UT, when it was shut down because of dawn. During this period no evidence of NLCs was found in the data, and they were not seen visually in the predawn twilight.

[9] On 24 June UT the lidar obtained good data between 0422 and 1108 UT. The NLC was most prominent during the first hour. This detection is shown in terms of backscatter ratio [e.g., *Langer*

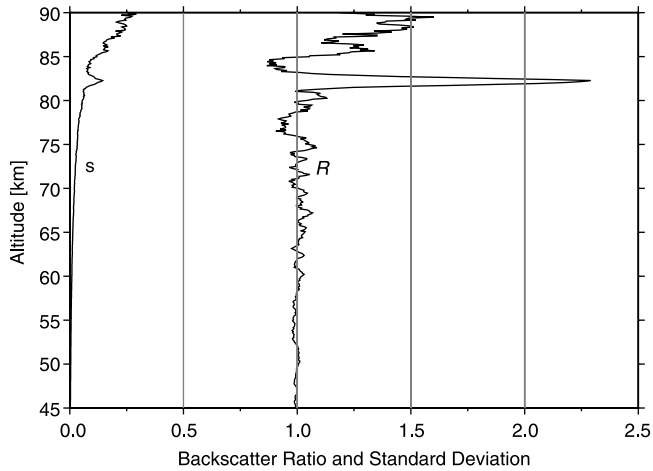

Figure 2. Lidar detection of a NLC at 82 km above Logan, Utah, on the evening of 23 June 1999 MDT. The backscatter ratio R for Δh = 675 m and Δt = 1 hour (10:22–11:22 P.M. MDT or, equivalently, 0422–0522 UT on 24 June 1999) is plotted along with one standard deviation s for the derived backscatter ratio. The Rayleigh-scatter reference curve needed to calculate R was derived from 4 hours of observations later the same night, when no aerosol scattering was apparent.

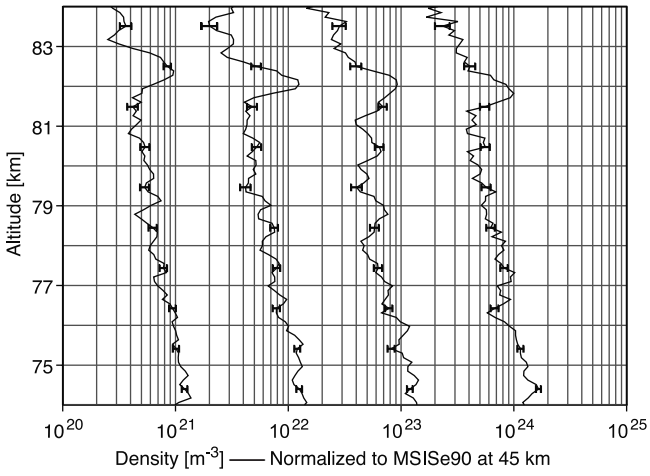

Figure 3. Comparison of the NLC and Rayleigh-equivalent signals. Four lidar profiles, for Δh = 338 m and Δt = 14 min on 23 June 1999 MDT starting at 10:22 P.M. MDT (midtime, 10:29 P.M.) or, equivalently, 0422 UT on 24 June 1999 (midtime, 0429 UT) are presented as neutral density. The abscissa applies to the leftmost profile. Each successive profile is shifted to the right by an order of magnitude. The NLC appears near 82 km: its peak signal is equivalent to the Rayleigh signal from 76 km, only 6 km lower. The neutral density at 82 km would be 4×10^{20} m^{-3}.

et al., 1995; *von Cossart et al.*, 1996] between 45 and 90 km in Figure 2. The backscatter ratio R is 1 for Rayleigh scatter and greater than 1 where aerosol scatter is present. The ''noisy'' curve is the R as a function of altitude for the 1-hour period 0422–0522 UT (102°–108° SZA) and for altitude smoothing of 675 m. Most of the data points are close to R = 1. The smoother curve near R = 0 gives the 1 standard deviation uncertainty for the observed R values. Apparent in the backscatter ratio profile are fluctuations for a small vertical scale that are consistent with the 1 standard deviation curve, fluctuations for a larger vertical scale that approach 4 standard deviations, and one large spike at ~82 km, the NLC. Although its 2.3-backscatter ratio is small, it is 9 standard deviations (or ~20 times the standard deviation for a R = 1 return). This is a highly significant detection, leaving no doubt that an aerosol-scattering layer was detected.

[10] To calculate this backscatter ratio profile a Rayleigh-scatter reference profile is needed. One was derived from the background-corrected count profile between 42 and 92 km, between 0608 and 1008 UT, when no detectable NLC backscatter signal appeared in the data. It differs from the curve with the NLC only in that its integration time is 4 times as long. It was then scaled to best match the 0422–0522 UT count profile between 45 and 60 km. The reference curve could equally well be determined with greater averaging in altitude or with a smooth curve, such as a polynomial, fitted to it. Our experiments with this have affected the NLC strength by ~10% and the peak altitude by approximately the quantization step of 112 m. The procedure followed here is the simplest. A detailed error-propagation calculation was performed to determine the 1 standard deviation values. It started from Poisson statistics for the two signal-plus-background count profiles and for the two background count measurements. The fluctuations pointed out above in the R profile can arise from fluctuations in either the data or the reference profile. In either case there is weak geophysical variability that exceeds the observational uncertainty. The length of the boxcar smoothing, for example, 338 m, 675 m, 1350 m, etc., applied to the data and reference profiles was varied to find the best compromise between reducing the noise fluctuations of the Rayleigh-scatter signal and showing the size of the aerosol-scattering layer. In Figure 2 the smoothing is over six data points, or 675 m, with a value shown every 112.5 m. Because the layer is thin and moving downward, as we shall see, the simple smoothing in time and altitude decreases the maximum backscatter ratio while increasing the area under the peak.

[11] In discussing NLC observations, absolute altitudes may become important: they have been reported with an apparent accuracy of 100 m and can be measured with an even greater accuracy. Yet the zero-altitude reference is rarely, if ever, specified and depending on its origin could have a significant error. With the advance of GPS technology, it is now feasible to determine lidar altitudes extremely accurately and to reference them to a common global geoid. We determined our location using a real-time kinematic GPS measurement, which was referenced to the World Geodetic System (WGS-84) ellipsoid and the WGS-84 Earth Gravitational Model 1996 (EGM96) global geoid [*National Imagery and Mapping Agency*, 2000]. Thus, with far more accuracy than needed for this study, the ALO laser is currently located 1465.8 m above this global reference surface.

[12] Figure 3 provides the most direct way of examining the NLC signal: it does not require a reference Rayleigh-backscatter profile. The lidar returns for Δh = 337.5 m and Δt = 14 min, starting at 0422 UT on 24 June 1999, are presented as atmospheric density profiles between 74 and 84 km. Also included are error bars representing plus and minus 1 standard deviation. The abscissa applies to the first profile, the leftmost one. For clarity, each successive 14-min profile is shifted to the right by an order of magnitude in density. The background-corrected signal was converted to density by multiplying it by range-squared and normalizing it to the Mass Spectrometer Incoherent Scatter model (MSISe90) [*Hedin*, 1991] at 45 km. The NLC stands out clearly from the density profile at ~82 km in the four time intervals. The underlying density is used in section 3 to derive the volume backscatter coefficient for aerosol scatter. The signal from the peak of the NLC layer is equivalent to the range-corrected Rayleigh-scatter signal at ~76 km, only 6 km lower.

[13] In Figure 4, six profiles of backscatter ratio R for Δh = 337.5 m and Δt = 12 min, starting at 0422 UT on 24 June 1999, are presented between 80 and 84 km as solid lines along with plus and minus 1 standard deviation error bars. (The reference curve was the same as that used for Figure 2, except that Δh was also reduced to

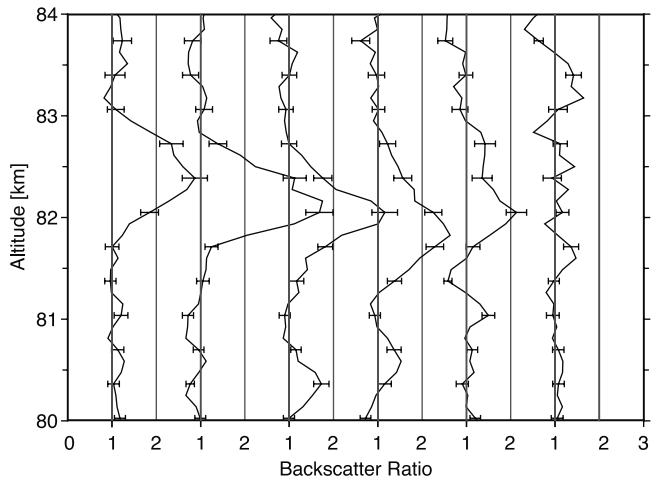

Figure 4. High-resolution profiles of backscatter ratio for the NLC layer. The backscatter ratios are shown for Δh = 338 m and Δt = 12 min on 23 June 1999 MDT starting at 10:22 P.M. MDT (midtime, 10:28 P.M.) or, equivalently, on 24 June 1999 UT starting at 0422 UT (midtime, 0428 UT). After the first profile each successive one is shifted to the right by the equivalent of two units in backscatter ratio. The first five profiles clearly show changes in the strength, altitude, and width of the NLC.

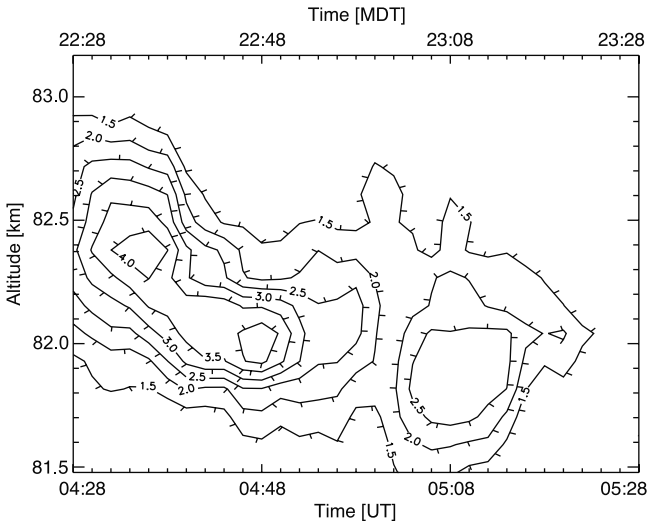

Figure 5. Time variations of the NLC observed at ALO on 23 June 1999 MDT. A contour plot of backscatter ratios is constructed from data obtained for Δh = 338 m and Δt = 12 min on 23 June 1999 MDT. The first integration started at 10:22 P.M. MDT (midtime, 10:28 P.M.) or, equivalently, on 24 June 1999 UT starting at 0422 UT (midtime, 0428 UT), and each successive one started 2 min later. The contours have small "spines" indicating the direction of decreasing backscatter ratio. The contours show the time evolution of the strength, altitude, and width of the NLC.

337.5 m.) Each profile has its own R = 1 and R = 2 abscissa values, and each is shifted by R = 2 to the right from the preceding one. The center time for the first curve is 0428 UT, for the second it is 0440 UT, and so forth. These profiles show time variability in the strength, altitude, and thickness of the NLC layer. The first four profiles show the layer descending, then ascending in the next profile before vanishing. The strength increases to a maximum R of 2.75 in the second profile and then decreases. Provided the observed profiles result from the convolution of the square 337.5-m sampling window with a square layer of thickness equal to or greater than the sampling window, then the full width at half maximum (FWHM) is a good measure of that thickness. The layer starts with a large FWHM, becomes thinner for each of the next two profiles, thickens for one profile, and then thins and vanishes.

[14] This time variation of the NLC strength, altitude, and width is shown more clearly and in more detail in Figure 5, a contour plot of backscatter ratio. It is obtained from a series of 12-min integrations, like those in Figure 4 and with the first center time at 0428 UT, but with each successive integration starting 2-min later. The smallest contour shown is for R = 1.5, with each level increasing by 0.5 until a maximum of R = 4.0 is reached. Initially, the NLC altitude is 82.4 km, the thickness is close to 800 m, and R is strong and increasing. It reaches ~4.4 at 0436 UT. It then descends rapidly, thinning to almost 400 m, and nearly attains R = 4.4 again by 0448 UT. After that, the backscatter ratio decreases erratically until ~0502 UT, recovers briefly, and then drops below the 1.5 contour by 0526 UT. As the backscatter ratio decreases, the layer ascends and becomes thicker. At it recovers, the layer descends and becomes thinner.

[15] Looking at its average behavior between ~0434 and 0508 UT, the NLC descends 0.55 km, giving an apparent average descent rate of 1.0 km h^{-1} or 27 cm s^{-1}, and then ascends 0.22 km. Without spatial observations or wind observations, we cannot determine whether this descent reflects a true descent or the effect of advecting a tilted layer through the lidar field of view. However, the rapid increases as well as decreases in backscatter ratio combined with the visible structure, albeit poleward of the lidar, strongly suggest that advection is important for the apparent vertical motion.

3. Discussion

[16] Although not previously seen at this low a latitude, the visual and lidar observations from Logan of the NLC are very similar to observations made at higher latitudes. The observations, occurring 1 and 2 days after summer solstice, are very near the middle of the NLC season, which appears to become shorter at more equatorward latitudes [e.g., *von Cossart et al.*, 1996]. The visual observations occurred toward the north between 97° and 105° local SZA, which is within the usual range for clouds between 80- and 85-km altitude and 3°–5° poleward. The smaller SZA gives rise to a high enough shadow height that the local sky is sufficiently dark for the clouds to be visible. The larger angle is related to how low to the horizon the clouds can be seen. The visible structure evident in Figure 1 is typical of most NLC observations.

[17] The visual observations, especially on 2 successive days, rule out other phenomena such as rocket exhaust plumes and meteoritic debris that the point measurements of the lidar would have difficulty discriminating against. The lidar observations then provide detailed characteristics of the cloud to compare to those determined from NLCs at higher latitudes.

[18] The strength of the backscattered lidar signal is a key characteristic: it can be described in several ways. The most direct way is by R, for which a maximum value of 4.4 was found. A less direct measure, because it depends on the neutral density, is the volume backscatter coefficient for aerosol scatter β_M. From R = 4.4 it is 3.4 times the volume backscatter coefficient for Rayleigh scatter, which makes it 0.85×10^{-10} m^{-1} sr^{-1}, using a neutral density of 4.0×10^{20} m^{-3} at 82 km and a Rayleigh-scatter cross section of 6.24×10^{-32} m^2 sr^{-1}. A related measure of the strength is the integrated backscatter coefficient, which is β_M integrated over the layer. This is approximated by multiplying β_M by the FWHM of the layer. Using the average value, 600 m, this gives an integrated β_M of 5.1×10^{-8} sr^{-1}. A final measure is the height of the range-corrected Rayleigh-equivalent altitude h_R. As shown in Figure 3, h_R is 76 km, just 6 km below the NLC. These four measures of the maximum strength of the layer and the other characteristics of the observed NLC at ALO are summarized in Table 1.

[19] The strength of the ALO NLC compared to the strength of NLCs measured elsewhere is given in Table 2. The strength parameters are listed in the first column. The last of these, $h_{NLC} - h_R$, is the altitude difference between the NLC and the range-corrected Rayleigh-equivalent altitude. The ALO NLC values are listed in the second column. Values from strong NLCs are given in the third and fourth columns, and values from weak NLCs are given in the fifth and sixth columns. The reference numbers refer to the locations and bibliographic references, which are given at the

Table 1. NLC Characteristics at ALO on 23 June 1999 MDT[a]

Characteristic	Value
Maximum backscatter ratio R,	4.4 at 82.4 km
Maximum volume backscatter coefficient, β_M, m^{-1} sr^{-1}	0.85×10^{-10}
Maximum integrated backscatter coefficient, sr^{-1}	5.1×10^{-8}
Range-corrected Rayleigh altitude h_R, km	76
Altitude range of peak, km	81.8–82.4
Cloud thickness (FWHM), m	400–800 m
Rate of descent, km h^{-1}	1.0 (27 cm s^{-1})

[a] NLC, noctilucent cloud; ALO, Atmospheric Lidar Observatory; FWHM, full width at half maximum.

Table 2. Comparison of NLC Strengths

Parameter	ALO NLC	Strong NLCs		Weak NLCs	
	Value	Value	Reference[a]	Value	Reference[a]
R	4.4	100–450	1	3–7	2
		240	2	6–14	6
		62–250	3	2	5
		70–161	4		
		18–20	5		
β_M, m^{-1} sr^{-1}	0.85×10^{-10}	$12–65 \times 10^{-10}$	3		
		$11–38 \times 10^{-10}$	4		
Integrated β_M, sr^{-1}	5.1×10^{-8}	$100–200 \times 10^{-8}$	2	$9–13 \times 10^{-8}$	7
h_R, km	76	41	2		
		~48–60	3		
$h_{NLC} - h_R$, km	6			5–10	2
				5–10	7

[a] References are as follows: 1, Andoya [*Hansen et al.*, 1989]; 2, Andoya [*Langer et al.*, 1995]; 3, Sondrestrom [*Thayer et al.*, 1995]; 4, Artic Lidar Observatory for Middle Atmosphere Research (ALOMAR) [*von Cossart et al.*, 1999]; 5, Juliusruh [*von Cossart et al.*, 1996]; 6, ALOMAR [*von Zahn et al.*, 1998]; 7, Aberystwyth [*Thomas et al.*, 1994].

bottom of Table 2. If the Sondrestrom values of h_R were range corrected, like the others, they would be at an even lower altitude. The detection of weak NLCs at high latitude is limited because of the much greater sky brightness during the NLC season than at midlatitudes [*von Zahn et al.*, 1998; J. P. Thayer, private communication, December 1999]. By any of these measures, a wide range of NLC strengths have been observed, and the ALO observations are at the very weak end of the range.

[20] The observed altitude of the ALO NLC appears low but within the range of the higher latitude reports, for example, at Andoya by *Hansen et al.* [1989] (82.2–83.4 km) and by *Langer et al.* [1995] (81–87 km), at ALOMAR by *von Cossart et al.* [1999] (81.4–84.6 km), at Sondrestrom by *Thayer et al.* [1995] (81.1–84.5 km), at Aberystwyth by *Thomas et al.* [1994] (83.0–86.5 km), and at Juliusruh by *von Cossart et al.* [1996] (81.0–86.0 km). However, because of the lowness of the ALO observations, we examined ellipsoids and geoids and made a careful measurement of the altitude of our laser. That did not account for the difference. More insight into NLC altitudes comes from the most extensive set of high-latitude observations, those from ALOMAR reported by *von Zahn et al.* [1998]. They show 34% of their mean hourly centroid altitudes in 1997 occurring between 81.5 and 82.5 km and 51% occurring between 82.5 and 86.5 km. This distribution says that most observations will have NLCs at a higher altitude than ours but that our small altitude range is the most likely.

[21] The observed thicknesses of the ALO NLC are within the range observed elsewhere but near the thin end. They are thicker than the thinnest layers measured elsewhere, for example, at Andoya by *Hansen et al.* [1989] (0.3 km). They are significantly thinner than many of the measurements, for example, at Andoya by *Hansen et al.* [1989] (1.4 km) and by *Langer et al.* [1995] (2.0–2.5 km), at Sondrestrom by *Thayer et al.* [1995] (2.0 km), and at Aberystwyth by *Thomas et al.*, [1994] (1.5–2.0 km). However, some of these latter layers may appear to be thick because of long integration times and vertical motion.

[22] The ALO NLC descent rate is within the range of downward rates deduced at Andoya by *Hansen et al.* [1989] (167 cm s^{-1}), at Sondrestrom by *Thayer et al.* [1995] (167 cm s^{-1}), at Aberystwyth by *Thomas et al.* [1994] (20 and 55 cm s^{-1}), and at ALOMAR by *von Zahn et al.* [1998] (9 cm s^{-1}). All these rates, except the last one, were derived from the observed descent of individual layers over an hour or two. As such, they represent maximum descent rates. Other time periods would provide descent rates approaching zero or, even, ascending rates. The last rate was derived from the tidal analysis of the extensive data set at ALOMAR. Thus the ALO rate is greater than the tidal rate but well within the observed range for individual NLCs.

4. Conclusions

[23] Most importantly, the combination of visual and lidar observations provides unequivocal evidence for the existence of a noctilucent cloud at 41.7°N, which is further equatorward than any previously reported sightings. The visual characteristics agree well with what has been observed over the last century, and the lidar-derived characteristics show this to be one of the weakest NLCs ever observed, to be near the lowest altitudes previously seen, and to be among the thinnest.

[24] The visual and lidar detections are ~8° and 11°, respectively, further equatorward than previously reported. Thus NLCs have gone from being a high-latitude phenomenon to also being a midlatitude one. The lidar observations show that this is a very weak, low, and thin NLC. These characteristics are consistent with the equatorward edge of a NLC.

[25] This midlatitude detection is significant because of what it may signify about global change. As discussed by *Thomas* [1996], it could occur because of an increase in greenhouse gases that cool the mesosphere, an increase in methane that would lead to more water vapor in the upper mesosphere, or a combination of the two. Less directly, it could also occur if there were an increase in the meridional circulation, perhaps because of an increased generation of gravity waves, leading to greater adiabatic cooling in the summer hemisphere (and warming in the winter hemisphere) or if there were significant temperature oscillations with a minimum at 82 km. In that regard, 1999 was a year with unusual weather that might have given rise to the generation of more gravity waves. Furthermore, these observations occurred over the Rocky Mountains, which is a strong orographic gravity wave source. An increase in these waves reaching the mesosphere would lead to an increase in the zonal wave-drag force. This, in turn, would lead to an increase in the meridional circulation [e.g., *Holton and Alexander*, 2000]. Or, they could contribute to the generation of temperature waves in the mesosphere and a localized temperature minimum near 82 km.

[26] A significant question is whether these observations represent the first documented penetration on a NLC to below 42°N or whether they are the first detection of something that has been occurring for a long time. Because a midlatitude penetration was so unexpected, nobody had been making a systematic search, and very few experienced observers are located at these latitudes. Similarly, very few Rayleigh-scatter lidars exist at these latitudes with enough sensitivity to observe the upper mesosphere and with

enough resources to observe on all clear nights. Furthermore, the twilight periods when NLCs can be visually detected become shorter as one moves equatorward, less than an hour near either dusk or dawn, and the NLC season appears to become shorter. In addition, this detection only occurred over a limited longitudinal region. Combining these factors, previous penetrations might have been missed, and future ones will be hard to detect without a concerted effort.

[27] Because of the potential adverse implications for global climate change, this midlatitude NLC observation demonstrates the need for systematic observations in the future from the USU mesospheric instrument cluster (ALO and Bear Lake Observatory), as well as from other sites. In addition to detecting the occurrence of these clouds, appropriate correlative observations need to be made to relate the occurrence to atmospheric chemistry and global dynamics. This includes observations of full temperature profiles from the stratosphere to the lower thermosphere, wind observations over as much of this profile as possible, and gravity wave observations.

[28] **Acknowledgments.** This research was supported in part by NSF CEDAR grants ATM9714789 and ATM9525815. It has benefited from useful discussions with Jeff Thayer, Timothy Kane, Gary Thomas, and David Rees. Lidar observations during 1999 were carried out by a dedicated group of students. In addition to the coauthors Joshua Herron and Bethany Martineau, this group included Brian Anderson, Will Fredin, Karen Marchant Nelson, Patrick Neary, and Marie Westbrook. The NLC was seen by three experienced NLC observers: one of the authors (Michael Taylor), the wife of another author (Gina Wickwar), and a colleague (Patrick Espy, private communication, December 1999). We thank Brian Atkinson of USU/SDL for combining two consecutive photographs to produce the panoramic photograph shown in Figure 1, and Helen Kenyon-Bares and Gary Mikkelson of Logan city for making the measurement used to precisely locate the lidar system.

References

Alpers, M., M. Gerding, J. Höffner, and U. von Zahn, NLC particle properties from a five-color lidar observation at 54°N, *J. Geophys. Res.*, *105*, 12,235–12,240, 2000.

Donahue, T. M., B. Guenther, and J. E. Blamont, Noctilucent clouds in daytime: Circumpolar particulate layers near the summer mesopause, *J. Atmos. Sci.*, *29*, 1205–1209, 1972.

Gadsden, M., and W. Schroder, *Noctilucent Clouds*, 190 pp., Springer-Verlag, New York, 1989.

Hansen, G., M. Serwazi, and U. von Zahn, First detection of a noctilucent cloud by lidar, *Geophys. Res. Lett.*, *16*, 1445–1448, 1989.

Hedin, A. E., Extension of the MSIS thermosphere model into the middle and lower atmosphere, *J. Geophys. Res.*, *96*, 1159–1172, 1991.

Holton, J. R., and M. J. Alexander, The role of waves in the transport circulation of the middle atmosphere, in *Atmospheric Science Across the Stratopause*, *Geophys. Monogr. Ser.*, vol. 123, edited by D. E. Siskind, S. D. Eckermann, and M. E. Summers, pp. 21–35, AGU, Washington, D.C., 2000.

Langer, M., K. P. Müller, and K. H. Fricke, Rayleigh lidar detection of aerosol echoes from noctilucent cloud altitudes at the Arctic circle, *Geophys. Res. Lett.*, *22*, 381–384, 1995.

National Imagery and Mapping Agency, Department of Defense World Geodetic System 1984: Its definition and relationships with local geodetic systems, *TR8350.2*, 3rd ed., amendment 1, Bethesda, Md., 2000.

Taylor, M. J., M. Gadsden, R. P. Lowe, M. S. Zalcik, and J. Brausch, Mesospheric cloud observations at unusually low latitudes, *J. Atmos. Sol. Terr. Phys.*, in press, 2002.

Thayer, J. P., N. Nielsen, and J. Jacobsen, Noctilucent cloud observations over Greenland by a Rayleigh lidar, *Geophys. Res. Lett.*, *22*, 2961–2964, 1995.

Thomas, G. E., Is the polar mesosphere the miner's canary of global change?, *Adv. Space Res.*, *18*(3), 49–58, 1996.

Thomas, G. E., and J. J. Olivero, Climatology of polar mesospheric clouds, 2, Further analysis of Solar Mesosphere Explorer data, *J. Geophys. Res.*, *94*, 14,673–14,681, 1989.

Thomas, L., A. K. P. Marsh, D. P. Wareing, and M. A. Hassan, Lidar observations of ice crystals associated with noctilucent clouds at middle latitudes, *Geophys. Res. Lett.*, *21*, 385–388, 1994.

von Cossart, G., P. Hoffmann, U. von Zahn, P. Keckhut, and A. Hauchecorne, Mid-latitude noctilucent cloud observations by lidar, *Geophys. Res. Lett.*, *23*, 2919–2922, 1996.

von Cossart, G., J. Fiedler, and U. von Zahn, Size distributions of NLC particles as determined from 3-color observations of NLC by groundbased lidar, *Geophys. Res. Lett.*, *26*, 1513–1516, 1999.

von Zahn, U., G. von Cossart, J. Fiedler, and D. Rees, Tidal variations of noctilucent clouds measured at 69°N latitude by groundbased lidar, *Geophys. Res. Lett.*, *25*, 1289–1292, 1998.

Wickwar, V. B., K. C. Beissner, T. D. Wilkerson, S. C. Collins, J. M. Maloney, J. W. Meriwether, and X. Gao, Climatology of mesospheric temperature profiles observed with the Consortium Rayleigh-scatter lidar at Logan, Utah, in *Advances in Atmospheric Remote Sensing With Lidar*, edited by A. Ansmann et al., pp. 557–560, Springer-Verlag, New York, 1997.

Wickwar, V. B., T. D. Wilkerson, M. Hammond, J. P. Herron, Mesospheric temperature observations at the USU/CASS Atmospheric Lidar Observatory (ALO), in *Lidar Remote Sensing for Industry and Environment Monitoring*, edited by U. N. Singh, T. Itabe, and N. Sugimoto, *Proc. SPIE*, *4153*, 272–284, 2001.

J. P. Herron, B. A. Martineau, M. J. Taylor, and V. B. Wickwar, Center for Atmospheric and Space Sciences, Utah State University, 4405 Old Main Hill, Logan, UT 84322-4405, USA. (sll5d@cc.usu.edu; mtaylor@cc.usu.edu; wickwar@aeronomy.cass.usu.edu)

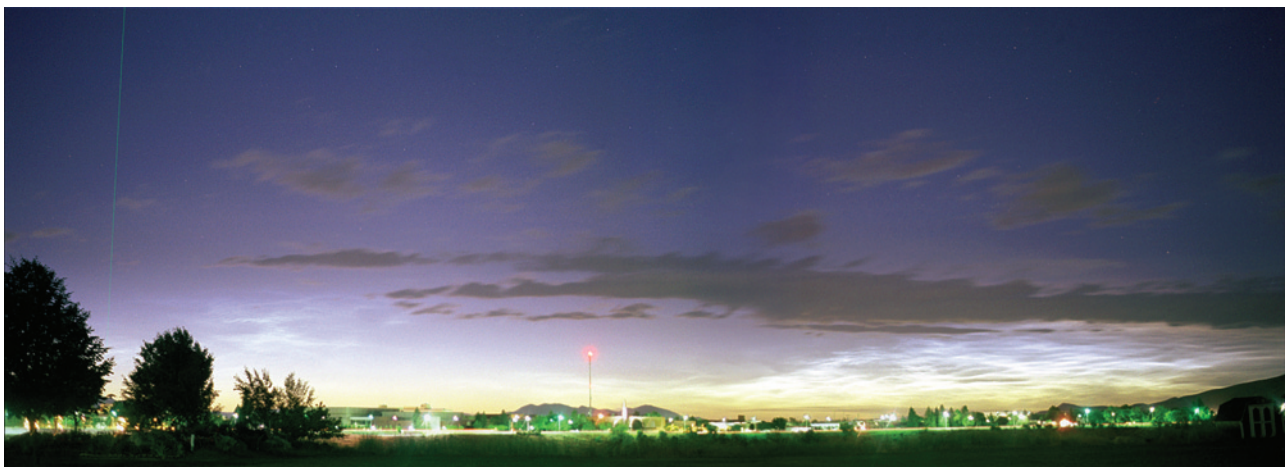

Figure 1. Panoramic photograph of noctilucent clouds (NLCs) from Logan, Utah, at 10:30 P.M. MDT on 22 June 1999 (0430 UT on 23 June 1999). The photograph (taken by one of the authors, M. J. Taylor) was obtained using a Minolta SLR fitted with a 50 mm, $f/1.7$ lens, and Kodak 100 ASA color film exposed for $\sim$10 s.